18TH WORLD CONFERENCE ON EARTHQUAKE ENGINEERING
WCEE2024
MILAN

MILAN, ITALY
30TH JUNE - 5TH JULY 2024
www.wcee2024.it

NEAR-REAL-TIME FRAMEWORK FOR SEISMIC PERFORMANCE CHARACTERIZATION OF A LARGE PORTFOLIO OF BUILDINGS

Aidin Tamhidi[1], Yousef Bozorgnia[2]

[1] Berkshire Hathaway Specialty Insurance, Catastrophe Engineering and Analytics, San Ramon, USA, aidin.tamhidi@bhspecialty.com

[2] Civil and Environmental Engineering Department, University of California, Los Angeles, USA

Abstract*: The traditional post-earthquake damage assessment of buildings is done visually through building-by-building inspections, which for a major event might take months to be completed. The main goal of this study is to establish a near-real-time framework to quantify the post-event seismic performance of a portfolio of soft-story (SS) residential buildings. Two main ingredients are required; 1) input ground motion time-series at the sites of the buildings that excite the structures, and 2) well-established nonlinear structural computer models representing the buildings. By having these two ingredients, nonlinear dynamic analyses of the existing structures can be performed, and the seismic performance of the portfolio buildings can be quantified. The first ingredient is provided by a previously established Gaussian Process Regression (GPR) model by Tamhidi et al. (2021). This GPR model generates ground motion time series at un-instrumented target sites (i.e., the sites of the buildings) employing the surrounding recorded ground motions. There is an inventory of OpenSees models constructed to represent approximately the 13,500 SS buildings in Los Angeles. This inventory includes thirty-two models categorized through four main features: first-story wall layout, the number of stories, floor plan dimension, and wood-frame shear wall material. We utilized visual recognition methodologies through machine learning (ML) to classify the first two features of the target SS buildings. The trained ML models were previously tuned by Tamhidi et al. (2022). The OpenStreetMap (OSM) is then used to detect the floor plan area of the target buildings to classify the third required feature. The "closest" available OpenSees model for each building is eventually chosen to complete the second ingredient of the framework. Having both a structural model and input ground motion time series, one can conduct a nonlinear response history analysis to assess the seismic performance of each specific building. As an application of the framework, ground motion time series at over 2,000 SS buildings' locations within Los Angeles for scenario* ***M****6.7 earthquake are generated. The structural features are also classified by trained ML model utilizing the Google Street View extracted images of the SS building. A map of the estimated damage state for the 2,000 SS buildings is produced, which demonstrates that more than 50% of the SS buildings are either severely damaged or collapsed after such an earthquake in Los Angeles while approximately 15% of them experienced slight damage.*

1. Introduction and Overview

The post-earthquake damage assessment of buildings can be very labor-intensive, judgmental, and time-consuming. For example, the inspection process took about two months to be completed for the 1994 Northridge earthquake (Trifunac and Todorovska, 1997). Thus, it is highly desirable to rapidly assess the building performance on an ultra-high scale within a region following a moderate-to-major earthquakes (see, e.g., Ranf et al., 2007; Earle et al., 2009; Mangalathu and Jeon, 2020). Such information can be utilized by government emergency first responders, stakeholders, state officials, building owners, and insurance companies to allocate their resources rapidly and efficiently. Many previous studies aimed to develop such framework employed the ground motion intensity measure (GMIM) combined with the building fragility curves to assess the damage state or performance of the buildings. However, a thorough nonlinear response history analysis of buildings using site-specific structural models and ground motion time series has less been accomplished.

Wood-frame buildings are among the most common types of dwellings in the United States cities. It is also very common that first stories of multi-unit wood-frame buildings are widely open for parking space or retails, which imposes an opening on the wall layout of the building. This opening within the first-story wall layout causes a considerable reduction in the lateral stiffness and strength of the first story compared to the immediate above story, resulting in a structural system known as a soft- and/or weak-story (SS) (FEMA P-807, 2012). Soft-story buildings are vulnerable to damage and possibly collapse during moderate to severe earthquake shakings (e.g., Holmes and Sommers, 1996). As an illustration, about two-thirds of 49,000 collapsed or damaged buildings in Los Angeles due to the 1994 **M**6.7 Northridge earthquake were soft-story structures (Public Policy Institute of California, 2006). A timely assessment of the distribution of damages to these vulnerable buildings requires two main components: 1) input ground motion time-series exciting at the location of the building, and 2) a reliable well-established computer structural model representing existing buildings. There are about 13,500 soft, weak, and open front (SWOF) buildings identified in Los Angeles metropolitan area in 2016 (Los Angeles Times, 2016). In this study, a framework for a near-real-time damage assessment of approximately 2,000 SS buildings in Los Angeles is presented through generating the two required mentioned components.

2. Methodology and Scope

In this Section, the utilized methodology to provide the two key components are presented. As the first component matters, the exciting ground motion time series at the target locations, Tamhidi et al. (2021) established a methodology to generate the input ground motion time series at the building locations where there are no recording instruments. In addition, the uncertainty quantification of these simulated ground motions is performed by Tamhidi et al (2023). For the second component, a total of thirty-two archetypical building models were developed by Burton et al. (2019) to represent 13,500 identified SS buildings within Los Angeles. It is aimed to identify the main features required to develop the “closest” structural model for each target SS building and to do so, an automated methodology to extract buildings’ images from Google Street View (GSV) service is developed. Then, these images are used to train Convolutional Neural Networks (CNNs) to detect and classify the main key components of the SS buildings through image recognition. Eventually, a **M**6.7 scenario earthquake is simulated by amplification of previously recorded ground motions for the 2020 **M**4.5 South El Monte earthquake in Los Angeles and the entire framework is implemented and evaluated.

2.1 Soft-Story Structural Models for Los Angeles

Burton et al. (2019) developed archetypical *OpenSees* structural models to represent SWOF buildings in Los Angeles by surveying 3,000 of them. They considered four first-story wall layouts for the SWOF buildings which are called L1, L2, L3, and L4, respectively and are shown in Figure 1. The L1 has one completely open wall line in the shorter direction and two partially open wall lines in the longer direction. In contrast, the L2 has a completely open wall line in the longer direction and two partially open ones in the shorter direction. L3 has one single open wall line surrounded by three walls, and L4 has two partially open wall lines. The 3000 surveyed SWOF buildings by Burton et al. have revealed that 72% and 23% are two and three-story buildings, respectively, and about 5% have more than three stories. Thus, the constructed *OpenSees* models included only two and three-story buildings. In addition, two variations of floor plan dimensions based on the ratio of the length (L) to width (B) of the buildings are considered. The higher L/B and lower L/B are called large and small aspect ratios, respectively. Lastly, the exterior wall material is assumed to be stucco on the outside and either gypsum wallboard (GWB) or horizontal wood siding (HWS) inside. The interior wall materials are also considered to be constructed with either GWB or HWS on both sides. The features of the developed thirty-two SWOF building models can be found in Burton et al. (2019).

In the next Subsection, we will present how to use various sources including machine learning (ML) methodologies through computer vision to detect the four required described features for any SS target buildings to be able to assign the corresponding *OpenSees* model at that location of interest. For that purpose 2,681 buildings out of the Los Angeles SWOF buildings are randomly chosen to train the ML models.

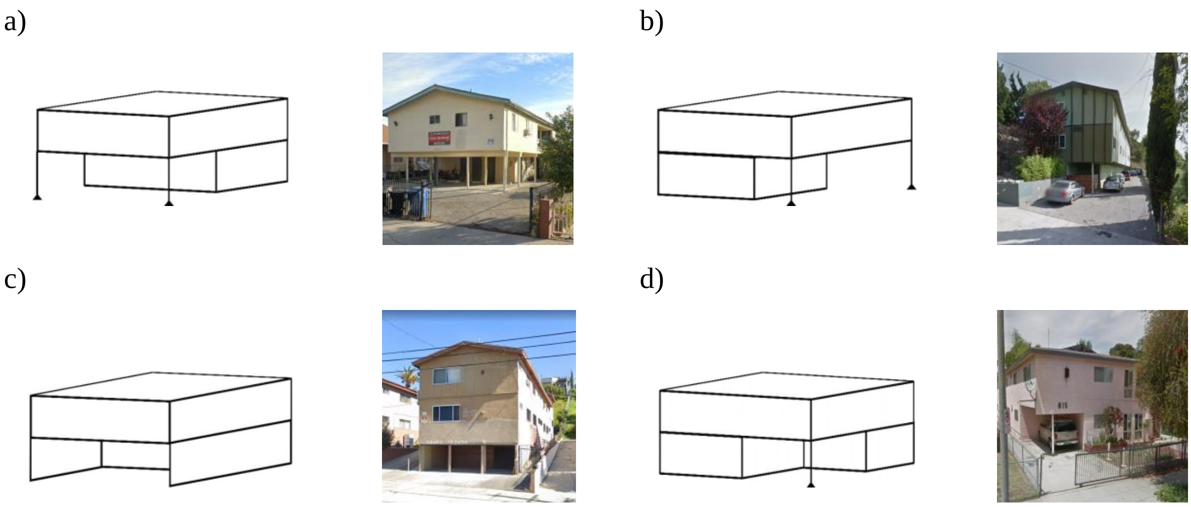

Figure 1. Schematic models for first-story wall layouts and their examples within Los Angeles SWOF wood frame buildings inventory for types a) L1, b) L2, c) L3, and d) L4

2.2 Buildings' Features Classification

The 2,681 randomly chosen buildings out of 13,641 identified SS buildings in Los Angeles are shown in Figure 2.a (blue points) to harvest the images out of GSV API to train CNN models for building features classifications. The GSV API returns one image from the closest available camera location on the street, given the coordinates of the building's center. This one collected image might not be sufficient to detect the opening of the first story due to various reasons, such as the occlusions from trees or trucks. In addition, there are many cases in which the opening of the first story is observable from side (back) streets or another viewpoint on the main street corresponding to their address. Therefore, we collected all available images within an 80m-radius of the building's center from different camera locations around the perimeter of the buildings using their corresponding calculated headings (Figure 2.b) to construct the image sets of the building. In addition, a fifth class, called L0, are defined to classify the buildings whose images cannot be fit into any of L1 through L4 classes. The detailed image harvesting and training procedure to classify the first-story wall layout of the buildings are described in Tamhidi 2022.

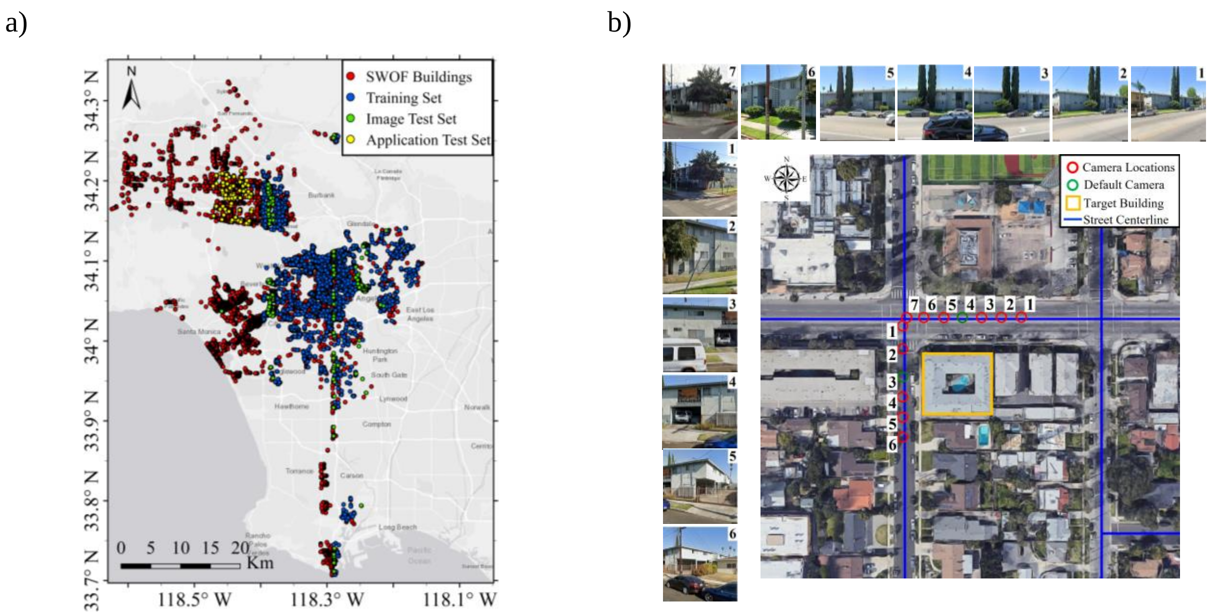

Figure 2.a) The distribution of the SWOF building inventory, training and test sets and b) Google Street View imaging parameters for building image collection described in Tamhidi (2022)

A set of 357 test buildings (green points in Figure 2.a) are picked to examine the performance of the trained CNN models. One image is obtained from each of the test buildings, which makes 357 and 350 images for soft-story wall layout and number of stories classification tasks, respectively. The distribution of the five classes for the first-story wall layout classification task in the test set is 23%, 26%, 6%, 26%, and 19%, for the classes L0 through L4, respectively and the similar distribution for the number of stories classification task is 78% and 22% for the two-story (2S) and three-story (3S) classes, respectively. As described by Tamhidi 2022, after training and validating multiple various CNNs models, the ResNet152 architecture (He et al., 2016) is chosen as the final model to be applied. Figure 3.a displays the confusion matrix, *C*, of the test set's predictions for the first-story wall layout classification. The confusion matrix element C_{ij} shows the recall for the i^{th} class, i.e., the fraction of i^{th} class images in the test set that is correctly labelled by the model. In Figure 3.a, the number of images constructed in each cell is shown in parentheses. As Figure 3.a depicts, the confusion matrix includes the maximum recall on its diagonal elements, which confirms the applicability of the trained model in detecting the first-story wall layout. A sample of correctly predicted classes within the image test set is provided in Figures 3b through 3e with the probability of the true estimated class (after applying the SoftMax function on the last layer of the CNN). In addition, Figures 3b through 3e include the Gradient-weighted Class Activation Maps (Grad-CAM) (Selvaraju et al., 2020) for a sample of images correctly classified in the image test set. Grad-CAM is a well-established methodology that utilizes the gradient information of a class activation with respect to different particles (pixels) of an image to produce a heatmap highlighting the regions essential for the classifier's decision about the estimated label. A similar approach is performed to evaluate the performance of the trained CNN model to estimate the number of stories of the target SS buildings. Tamhidi et al. (2022) demonstrated that the 91% and 94% of the true two-story and three-story buildings were labelled correctly.

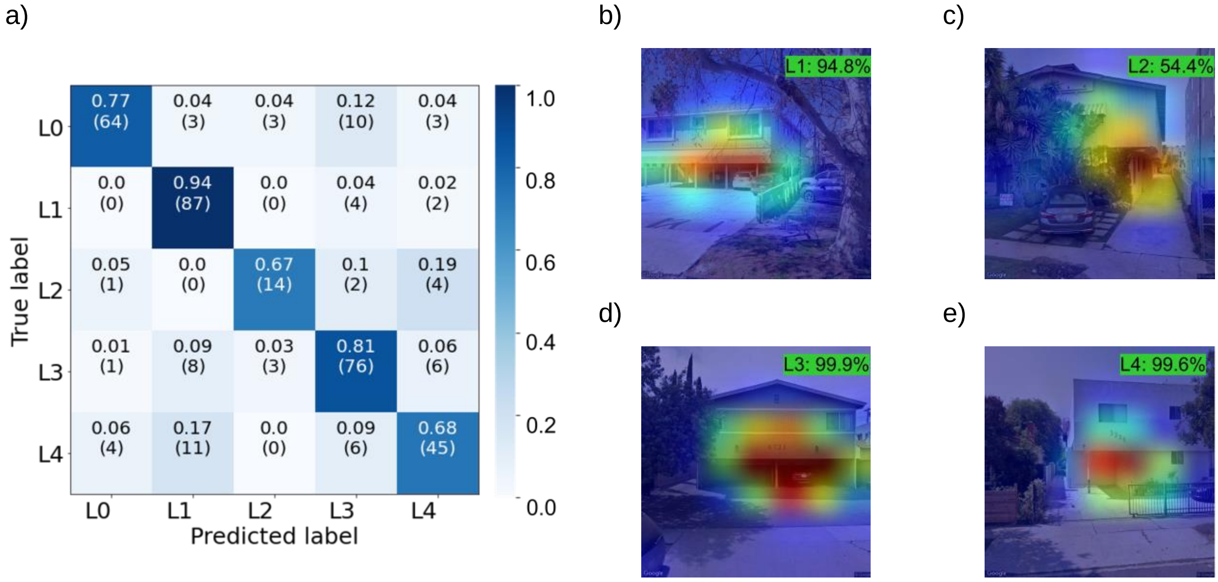

Figure 3.a) Confusion matrix for image test set of first story wall layout classification and correctly classified images and their Grad-CAM for class b) L1, c) L2, d) L3, and e) L4

The building's third feature, the floor plan dimension, must be chosen as either longer or shorter aspect ratio, as provided in Burton et al. (2019) (also c.f. Table 4.1 in Tamhidi 2022). To do so, we obtained the building's footprint coordinates from *OpenStreetMap* (OSM), providing geographical coordinates of urban facilities, including residential buildings. The buildings' floor plan area can then be calculated by having the coordinates of the footprints' vertices. We chose the plan dimension that constructs the closest area to the existing building's area. Thus, the total shear wall length would be close between the structural model and the actual building. Eventually, the last required component, the shear wall materials, remains unknown, for which we conduct analyses for both types of shear wall materials GWB and HWS. The whole procedure of the allocating *OpenSees* structural models at the target SS building locations is demonstrated in Tamhidi 2022 where interested readers may find the image level and building level performance evaluations of the methodology as well. Moreover, the ML performance is compared with human performance in detecting the required structural features in Tamhidi 2022.

3. Framework for Near-Real-Time Damage Assessment

In this study, the framework described in Section 2 is applied for a subset of 2,000 existing un-retrofitted SS structures in Los Angeles. It is worth mentioning that these randomly selected buildings are chosen outside of the training sets utilized for CNN models' training set. The combination of Community Seismic Network (CSN) and the California Integrated Seismic Network (CISN) recording sites is utilized to generate the ground motion time series at each of the SS buildings' locations. In this study, the following steps are taken to prepare and apply the developed framework:

- A **M**6.7 scenario earthquake is synthetically generated by amplifying the recorded ground motions of 2020 **M**4.5 South El Monte at CISN and CSN sites. The Bayless and Abrahamson (2019) (BA19) Fourier amplitude spectrum model is utilized to magnify the recorded motions.
- The GPR model established by Tamhidi et al. (2021) is utilized to generate the ground motion time series at each of the SS building's locations, given the CISN and CSN sites' amplified motions.
- The structural features, including first-story wall layout, number of stories, and floor plan dimension, are obtained using extracted GSV images and the OSM platform as described in Section 2. The closest *OpenSees* models (considering both wall materials) out of the thirty-two models is chosen for each SS building in the testbed.
- Nonlinear response history analyses for the 2,000 SS buildings are conducted using the simulated ground motions and the selected structural models. The damage state of the buildings is estimated using the structural responses.
- The distribution of the structural performances is plotted as a map where one can find which buildings are probably safe, severely damaged, or potentially collapsed.

Figure 4 schematically summarizes the whole framework described above to map the performance estimates of the chosen SS buildings in Los Angeles.

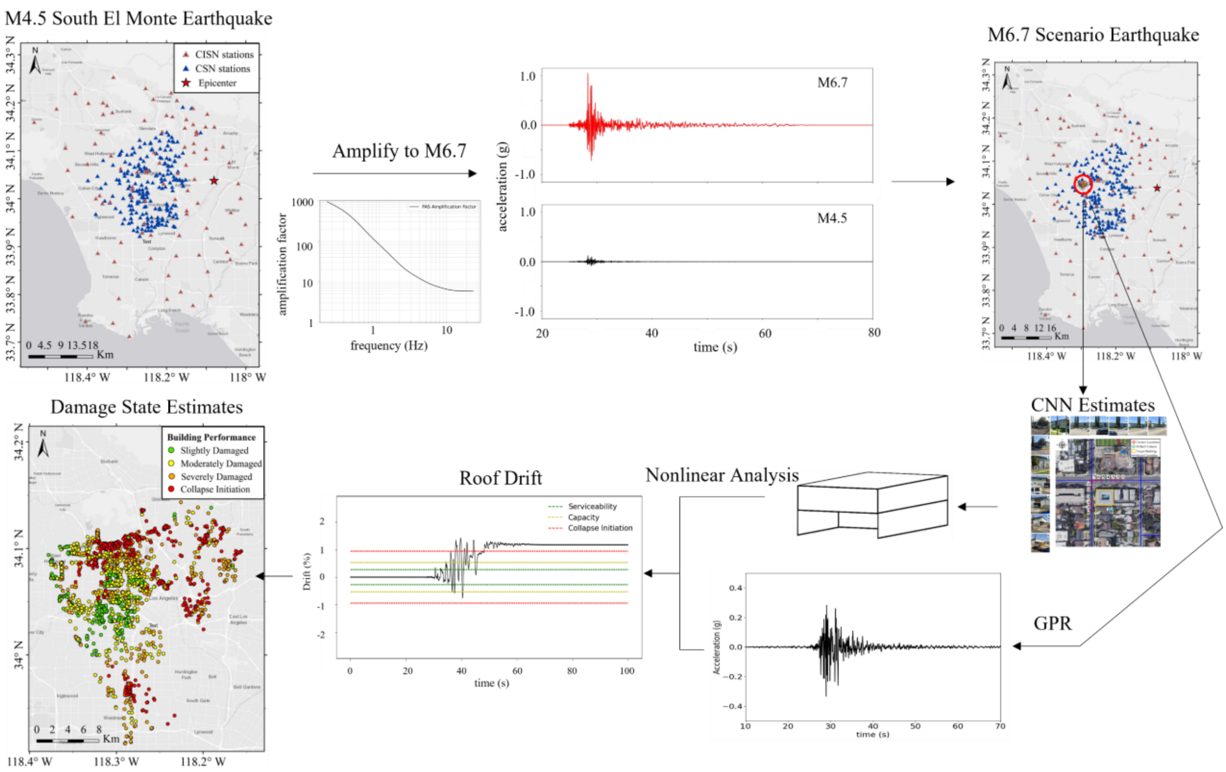

Figure 4. The schematic framework for estimating the damage state of the testbed SS buildings in Los Angeles

3.1 Ground Motion Simulation for a Scenario M6.7 Earthquake

The scenario **M**6.7 earthquake is constructed based on the point-source assumption, which does not consider finite fault, which is expected for an earthquake with magnitude 6.7. In this study, the BA19 model is utilized to simulate the effective amplitude spectrum (EAS) of the ground motions at each CISN and CSN station for the **M**4.5 South El Monte earthquake. Then, the EAS of the motions corresponding to a scenario **M**6.7 earthquake at the same sites are estimated through the same model. Eventually, the ratio between the two estimated EAS proposes the amplification factor. After amplifying the FAS of the motions, the initially recorded phase spectra are used to convert the Fourier Spectra to the time domain associated with the scenario **M**6.7 earthquake. The Z_{tor} for the South El Monte earthquake is assumed to be 14.0 km (about 3 km shallower than its hypocentral depth), while the Z_{tor} of the scenario earthquake is assumed to be 5 km (similar Z_{tor} for the Northridge earthquake based on USGS, 2013). The epicentre location of the scenario earthquake and faulting type are considered the same as those of the South El Monte earthquake. The $Z_{1.0}$, depth to the horizon with a shear-wave velocity of 1.0 Km/s, is estimated using the SCEC CVMS-4 model (Lee et al., 2014). The Vs_{30} of the sites are also predicted through the proxy-based model, as described in Ahdi et al. (2020).

Figure 5.a illustrates the location of the SS buildings with respect to the seismic network recording sites and Figure 5.b demonstrates a sample of **M**4.5 South El Monte recorded motion, the corresponding amplified **M**6.7 scenario earthquake simulated motions, and the amplification factors calculated through the ratio of EAS in BA19 model.

a) b)

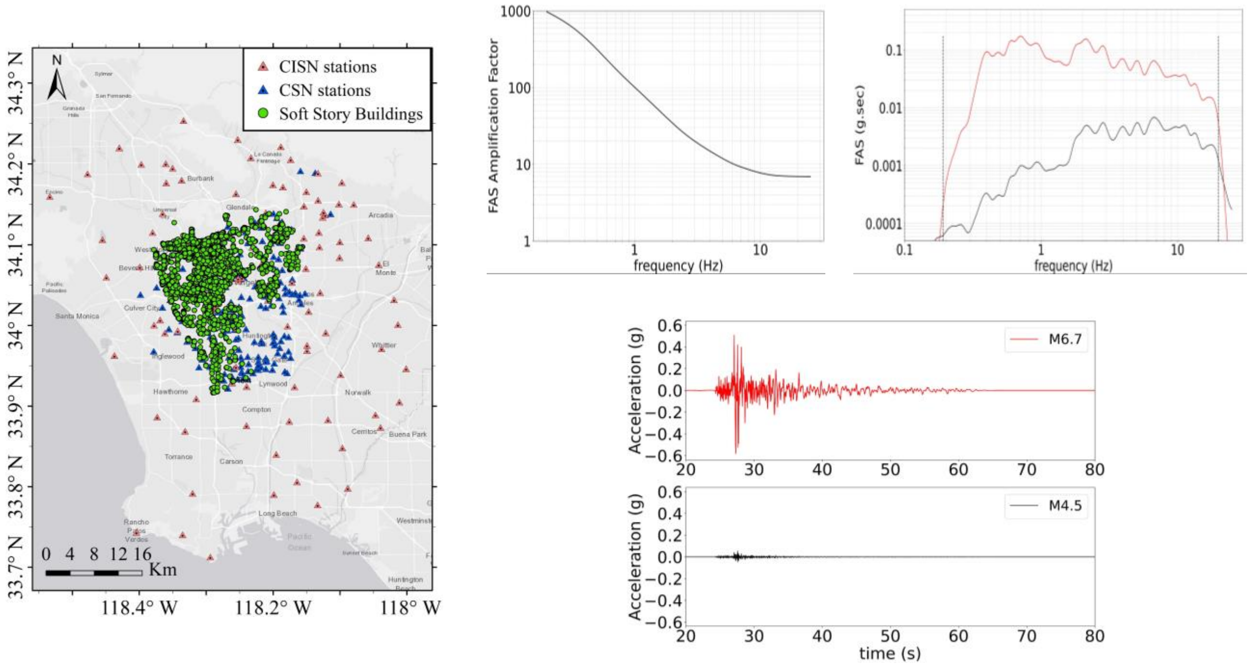

*Figure 5. a) The distribution of chosen Soft-Story buildings as testbed and CISN and CSN's recording sites in Los Angeles b) Frequency amplification factor, FAS, and ground motion time series for a sample of **M**6.7 scenario earthquake*

Eventually the ground motion time series at each of the 2000 SS building locations (cf. Figure 5.a) are generated for the **M**6.7 scenario earthquake utilizing the amplified recorded motions as the observation. Interested readers are referred to read Tamhidi 2022 to investigate more detailed information regarding the amplified ground motions for the **M**6.7 scenario earthquake in Los Angeles.

3.2 Structural Model Assignment

In this subsection, we present the allocation of the "closest" SS structural model to each of the selected SS buildings to be excited with the site-specific simulated ground motions elaborated in the previous subsection.

To do so, the images surrounding each testbed's buildings are extracted and fed to the trained CNN models described in Section 2. The algorithm shown in Figure 4 is utilized to label the building's first-story wall layout and the number of stories. Figure 6 demonstrates the prediction results for the first-story wall layout and number of stories classification for the 2000 SS buildings of the testbed.

a) b)

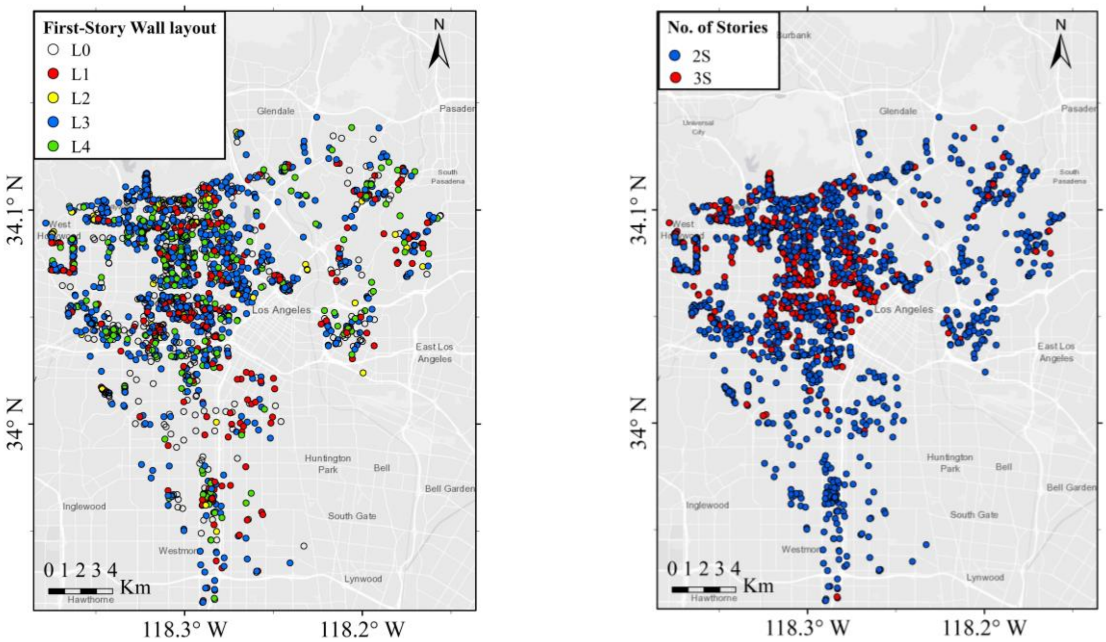

Figure 6. The prediction of a) first-story wall layout and b) number of stories for the chosen SS buildings as the testbed in Los Angeles using trained CNN models

In Figure 6.a, 475 buildings are labeled as L0, meaning that their harvested images are not sufficient to classify corresponding buildings as either L1 through L4 classes. In other words, about 25% of the 2000 testbed SS buildings are classified L0. About 21%, 4%, 56%, and 19% of the non-L0 class buildings are estimated as L1, L2, L3, and L4, respectively. The estimation results of the CNN model for the SS buildings are consistent with the survey results by Burton et al. (2019) study (17%, 2%, 61%, and 20% for L1, L2, L3, and L4 classes). This verifies that the trained CNN model estimation asserts the distribution of different first-story wall layout types with the in-person surveying of Los Angeles SS buildings.

In Figure 6.b, 76% and 24% of the SS buildings were classified as two-story and three-story buildings, respectively. The closest floor plan dimension has been assigned to each non-L0 building using the OSM input features. Both the Gypsum Wall Board and Horizontal Wood Siding material are considered as the material of the buildings, and both will be investigated through nonlinear response history analysis. For the buildings labeled as L0, all four first-story wall layout types with their closest corresponding dimension are used to estimate the structural responses.

3.3 Structural Damage State Estimates

The damage state levels are defined based on the drift limits (e.g., HAZUS, 2015). The pushover response of the structural models is commonly utilized to define the "capacities" for different performance levels of the structures. The drift limit states using pushover analysis are shown by (Yi, 2020) and are employed in this study. For that purpose, each SS structural model in *OpenSees* developed by Burton et al. (2019) is analysed through displacement control pushover along two orthogonal directions, called X and Y. The X direction refers to the longitudinal (longer) dimension of the floor plan, while the Y direction represents the transverse (shorter) one. The displacement control push-over analysis is performed to determine the drift limits in each direction of the developed structural *OpenSees* models. The chosen drift limits for the "Serviceability", "Capacity", and "Collapse Initiation" performance states are shown in Tamhidi et al (2022). The chosen drifts for the serviceability and collapse initiation correspond to the base shear equal to 80% of the strength capacity (ultimate strength). The drift corresponding to the maximum base shear, i.e., the ultimate strength, is picked as the drift associated with the capacity. Then, these drift limits are utilized to decide the damage state of the SS buildings in each direction. the majority of SS building models have an elastic drift limit, D_e, of around 0.3% in both horizontal directions. In both directions, the average collapse initiation (incipient) drift, D_p, is around 1.1%. It is noted that these building models are for un-retrofitted SS buildings. Retrofitted buildings, which are out of scope of the current study, are expected to have higher capacities. The two components required for the framework for performance characterization of chosen SS buildings are established. We determined the damage state of each SS building along the horizontal directions through the following steps:

- The first-story wall layout category of the target building is obtained from the CNN model's estimation.
- The number of stories is predicted by employing the CNN model (Figure 6b).
- The building area is obtained from the *OSM*, given the coordinates of the building. Then, the closest floor plan dimension out of the two plan aspect ratio choices is chosen such that the model's area become as close as possible to the actual building's area.
- The two *OpenSees* models corresponding to GWB and HWS wood-frame wall materials, given the three determined features in steps 1 through 3, are used to conduct the nonlinear response history analysis. The 3D *OpenSees* models are simultaneously excited, employing two horizontal components of ground motion time series. The structural responses, specifically the roof drift in two horizontal directions are recorded.
- The maximum roof drift during the excitation in each direction is recorded. Then, those maxima are compared to their corresponding drift limits. The damage state of the corresponding direction is considered as slight, moderate, severe, and collapse initiation if the maximum drift in that direction falls below D_e, between D_e and capacity drift, D_m, between D_m and D_p, and beyond D_p, respectively.

In Figure 6a, there are 475 SS buildings that are labeled as L0. For these buildings, each L1 through L4 model using the corresponding features (number of stories and floor plan dimension) is employed to perform the nonlinear response history analysis through the generated ground motions. Then, the damage state of each category is determined through the defined procedure above. Finally, the weighted average of damage states using the weights 0.29, 0.06, 0.45, and 0.20 for the categories L1, L2, L3, and L4, respectively, is calculated and rounded up to the closest worst condition. Therefore, all the 1,883 SS buildings' performance considering two types of GWB and HWS wood-frame wall material is determined. Figure 7 demonstrates the distribution of the 5%-damped RotD50 spectrum at T=0.2 s for the simulated ground motions as well as the estimated damage states considering GWB as the wood-frame shear wall materials.

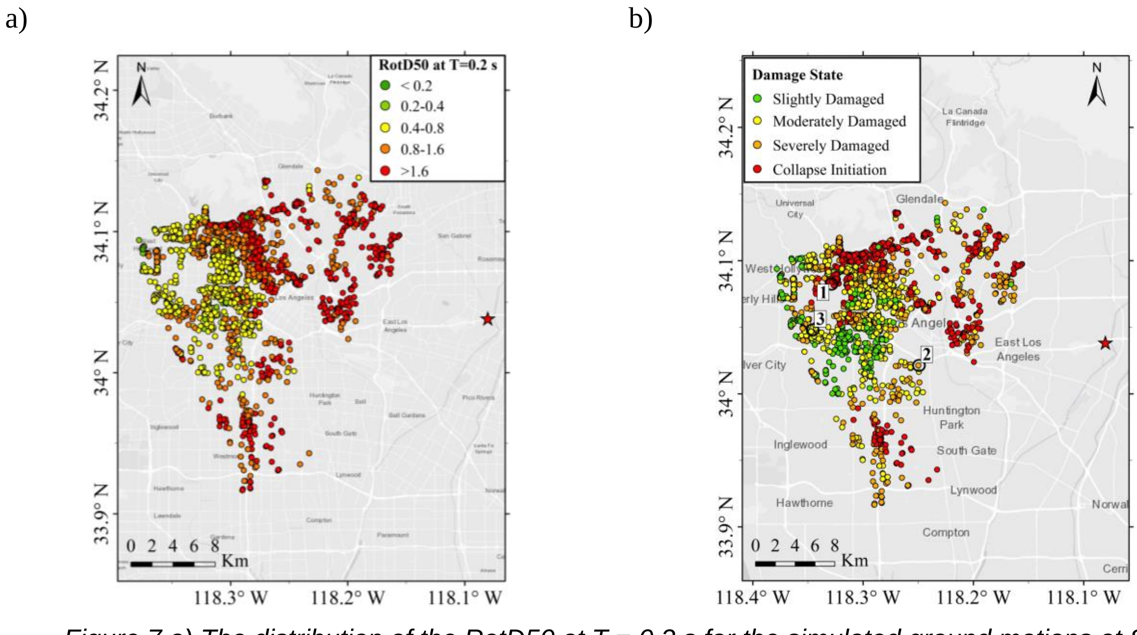

Figure 7 a) The distribution of the RotD50 at T = 0.2 s for the simulated ground motions at SS building's locations for scenario ***M****6.7 earthquake and b) The distribution of the estimated damage states for the testbed SS buildings with Gypsum Wall Board*

Table 1 summarizes the damage state of each building category for GWB considered wall material. In Table 1, the values within parentheses in front of the percentages demonstrate the number of buildings that falls in that partition. The percentage in each cell shows the portion of buildings inside each layout category.

Table 1. Damage state distribution among various categories with Gypsum Wall Board material

	Damage State			
	Slightly Damaged	Moderately Damaged	Severely Damaged	Collapse Initiation
L0	17.9%(85)	33.7%(160)	23.15%(110)	25.3%(120)
L1	9.3%(27)	29.3%(85)	27.6%(80)	33.8%(98)
L2	8.9%(5)	19.6%(11)	32.2%(18)	39.3%(22)
L3	17.4%(138)	33.7%(268)	25.3%(201)	23.6%(187)
L4	17.2%(46)	34.3%(92)	16.4%(44)	32.1%(86)
Total	**16%(301)**	**32.7%(616)**	**24%(453)**	**27.3%(513)**

Table 1 shows that generally about 52% of the SS buildings experienced either severely damaged or collapse initiation damage states after the scenario **M**6.7 local earthquake. In addition, it is concluded that just around 16% of the SS buildings experienced slight damage after the earthquake and, thus, approximately 85% of SS buildings experienced considerable damage. It is shown from Table 1 that L2 has the worst performance as it has the lowest percentage of slightly damaged buildings and the highest percentage of collapse initiations. On the other hand, it is shown that L3 had the best performance as it has a generally higher percentage of slightly damaged and lowest percentage of the collapse initiation damage states.

In summary, we demonstrated the whole framework's application for a large set of SS buildings in Los Angeles. The procedure including the ground motion time series simulation and nonlinear response history analyses of the SS buildings, is conducted on the University of California Los Angeles computational and storage services associated with the Hoffman2 Shared Cluster for Digital Research and Education's Research Technology Group. Using such computational power makes the whole framework rapid, as the nonlinear dynamic analyses process for about 2,000 SS buildings took about 30 minutes to be completed using 200 CPU cores.

4. Summary and Conclusion

The traditional post-earthquake damage assessment of structures is a labor-intensive and time-consuming process. Thus, many organizations, including government agencies, can benefit from a near-real-time seismic performance assessment. As the price of instrumentations becomes cheaper by passing the time, the future number of recording instruments will be much higher than those of today and cities will become densely instrumented, i.e., gradually becoming "smart" cities where highly dense granular recording instruments are installed outside and inside of structures. The main objective of this study was to provide the ingredients required for establishing a framework which can be utilized for the post-earthquake near-real-time seismic performance assessment of a large portfolio of structures, in this study for soft-story (SS) buildings. More precisely, the issues addressed in this study are presenting an automated methodology using image recognition techniques to establish the "closest" structural computer models for the existing SS buildings. The combination of the allocated structural models for each SS target building and also generating the ground motion exciting time series at the same location through the GPR model developed by Tamhidi et al (2021), the application of the near-real-time framework to estimate the damage states of the SS buildings for a major earthquake in Los Angeles is illustrated.

Acknowledgement

The study presented in this manuscript was supported by the University of California, Los Angeles (UCLA) Graduate Fellowship, National Science Foundation (award no. 2025310), California Department of Transportation, and Pacific Gas and Electric Company which are all appreciated. Any opinions, findings, conclusions, or recommendations expressed are those of mine and do not necessarily reflect those of supporting agencies. The helps from Dr. Nicolas Kuehn, Prof. Mohamad Alipour, Prof. Monica Kohler, Prof. Tadahiro Kishida, Prof. Pengfei Wang, Prof. Ertugrul Taciroglu, Dr. Zhengxiang Yi during this study are greatly appreciated.

References

Ahdi, S.K., Mazzoni, S., Kishida, T., Wang, P., Nweke, C.C., Kuehn, N.M., Contreras, V., Rowshandel, B., Stewart, J.P. and Bozorgnia, Y., 2020. Engineering characteristics of ground motions recorded in the 2019 Ridgecrest earthquake sequence. Bulletin of the Seismological Society of America, 110(4), pp.1474-1494.

Bayless, J. and Abrahamson, N.A., 2019. Summary of the BA18 Ground-Motion Model for Fourier Amplitude Spectra for Crustal Earthquakes in California. Bulletin of the Seismological Society of America, 109(5), pp.2088-2105.

Burton, H., Rad, A.R., Yi, Z., Gutierrez, D. and Ojuri, K., 2019. Seismic collapse performance of Los Angeles soft, weak, and open-front wall line woodframe structures retrofitted using different procedures. Bulletin of earthquake engineering, 17(4), pp.2059-2091.

Earle, P.S., Wald, D.J., Jaiswal, K.S., Allen, T.I., Hearne, M.G., Marano, K.D., Hotovec, A.J. and Fee, J.M., 2009. Prompt Assessment of Global Earthquakes for Response (PAGER): A system for rapidly determining the impact of earthquakes worldwide. US Geological Survey Open-File Report, 1131(2009), p.15.

FEMA P-807. 2012. “Seismic Evaluation and Retrofit of Multi-Unit Wood-Frame Buildings With Weak First Stories, FEMA P-807.” Federal Emergency Management Agency, Washington, DC., no. May: 336.

FEMA. 2015. “Technical and User’s Manual of Advanced Engineering Building Module (AEBM) ‘Hazus MH 2.1.’” Federal Emergency Management Agency.

He, K., Zhang, X., Ren, S. and Sun, J., 2016. Deep residual learning for image recognition. In Proceedings of the IEEE conference on computer vision and pattern recognition (pp. 770-778).

Holmes, W.T. and Somers, P., 1996. Steel Buildings. Northridge Earthquake of January 17, 1994, Reconnaissance Report, 2.

Lee, E.J., Chen, P., Jordan, T.H., Maechling, P.B., Denolle, M.A. and Beroza, G.C., 2014. Full-3-D tomography for crustal structure in southern California based on the scattering-integral and the adjoint-wavefield methods. Journal of Geophysical Research: Solid Earth, 119(8), pp.6421-6451.

Los Angeles City, Street Centerlines and Street Intersections in the City of Los Angeles. https://data.lacity.org/City-Infrastructure-Service-Requests/Street-Centerline/7j4e-nn4z.

Mangalathu, S. and Jeon, J.S., 2020. Ground motion-dependent rapid damage assessment of structures based on wavelet transform and image analysis techniques. Journal of structural engineering, 146(11), p.04020230.

Public Policy Institute of California, 2006, available at https://www.ppic.org/ (last accessed November 2022)

Ranf, R.T., Eberhard, M.O. and Malone, S., 2007. Post-earthquake prioritization of bridge inspections. Earthquake Spectra, 23(1), pp.131-146.

Selvaraju, R.R., Cogswell, M., Das, A., Vedantam, R., Parikh, D. and Batra, D., 2017. Grad-cam: Visual explanations from deep networks via gradient-based localization. In Proceedings of the IEEE international conference on computer vision (pp. 618-626).

Tamhidi, A., Kuehn, N., Ghahari, S.F., Rodgers, A.J., Kohler, M.D., Taciroglu, E. and Bozorgnia, Y., 2021. Conditioned Simulation of Ground-Motion Time Series at Uninstrumented Sites Using Gaussian Process Regression. Bulletin of the Seismological Society of America, 112(1), pp.331-347.

Tamhidi, A., 2022. Earthquake Resilient Smart Cities: A Framework for Collection and Utilization of Highly Granular Field Data for Seismic Performance Characterization of Soft-Story Buildings. University of California, Los Angeles.

Tamhidi, A., Kuehn, N.M. and Bozorgnia, Y., 2023. Uncertainty quantification of ground motion time series generated at uninstrumented sites. Earthquake Spectra, 39(1), pp.551-576.

Trifunac, M. D., and M. I. Todorovska. 1997. “Northridge, California, Earthquake of 1994: Density of Red-Tagged Buildings versus Peak Horizontal Velocity and Intensity of Shaking.” Soil Dynamics and Earthquake Engineering 16 (3): 209–22. https://doi.org/10.1016/S0267-7261(96)00043-7.

Yi, Z., 2020. Performance-based analytics-driven seismic retrofit of woodframe buildings. University of California, Los Angeles.